

Parametrical Approach for Modeling of Tire Forces and Torques in TMeasy 5

Dipl.-Ing. Ronnie Dessort, Dr.-Ing. Cornelius Chucholowski
TESIS DYNAware GmbH

Prof. Dr.-Ing. Georg Rill
OTH Regensburg

The final publication is available at link.springer.com via
http://dx.doi.org/10.1007/978-3-658-13255-2_31

1 TMeasy in a Nutshell

1.1 Introduction

For the dynamic simulation of on-road vehicles, the model-element “tire/road” is of special importance, according to its influence on the achievable results. Sufficient description of the interaction between tire and road is one of the most challenging tasks of vehicle modeling. Two groups of tire models can be classified: handling models and structural or high-frequency models. Usually, various assumptions are made in modeling vehicles as multibody systems. Therefore, in the interest of balanced modeling, the precision of the complete vehicle model should stand in reasonable relation to the performance of the applied tire model. Handling tire models are characterized by a useful compromise between user friendliness, model complexity, and efficiency in computation time on the one hand, and precision in representation on the other hand.

TMeasy represents a handling tire model based on a semi-physical model. It includes a massless force element acting between the road and the wheel. The unevenness of roads is approximated by small local planes in the contact region of the tire. TMeasy generates all components of the contact force vector and contact torque vector including a first order tire dynamics. The wheel modeled by a rigid body must incorporate mass and inertia properties of the rim and the tire. TMeasy is available as part of several commercial vehicle simulation packages like TESIS DYNAware products and is very successful used in handling applications – offline and in realtime.

TMeasy parameters are easy to guess: even with a crude knowledge of size, payload as well as friction property of the tire-road combination a first guess gives feasible results - good enough for simulation of extraordinary tires, [1]. Of course, the parameters can be adjusted by curve fits to meet given tire measurements or vehicle dynamic results more precise, [2]. Another advantage lies in the ease with which tire properties can be scaled to represent different road and tire conditions.

1.2 Wheel Position and Orientation, Axis Systems, Forces and Torques

The position vector r_{0C} and the unit vector e_{yR} represent the location and orientation of the wheel with respect to the earth-fixed axis system, Figure 1.

In normal driving situations, the contact patch between tire and road forms a coherent area and the effect of the pressure and tension distribution can be fully described by a resulting force vector applied at a specific point P of the contact patch and a torque vector. The vectors are described in a wheel-fixed axis system, which coincides with

the W-axis (Wheel-axis) system defined in the ISO-Directive 8855. The z_W -axis is normal to the local road plane. The x_W -axis is mutually perpendicular to the z_W -axis and to the wheel rotation axis e_{yR} and fixes also the third element of right-handed W-axis-system y_W . The components F_x , F_y , F_z of the contact force vector are named longitudinal force, lateral force, and normal force or wheel load according to the direction of the axes in the W-system. A cambered tire generates a tilting torque T_x around the x_W -axis. The non-symmetric distribution of the normal forces in the contact patch causes the torque T_y around the y_W -axis which is responsible for the rolling resistance. The irregular distribution of shear stress caused by friction in the road plane induce a torque T_z around the z_W -axis, which in particular is important in vehicle dynamics and is induced by two main effects $T_z = T_B + T_S$. The bore or turn torque T_B is generated by drilling the tire around the z_W -axis perpendicular to the footprint like in a parking maneuver. The self-aligning torque T_S is mainly induced by lateral force, because the center of the friction tension does not coincide with the geometrically defined contact point P.

TMeasy provides the resulting tire force and torque vectors F_C and T_C applied at the wheel center C as an interface to multibody systems.

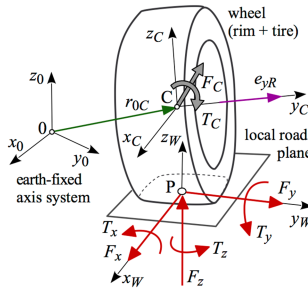


Figure 1: Axis systems, forces and torques

1.3 Contact Geometry

The calculation of the geometric contact point is an important part of TMeasy since it takes the shape of the tire and the road plane into account.

The track may have irregularities described by an arbitrary function of two spatial coordinates, $z = z(x;y)$. The current position of the wheel center C and the unit vector e_{yR} of the wheel rotation axis are known, Figure 2. On an uneven track, the contact point P cannot be calculated directly. Four points P_1 and P_2 as well as P_3 and P_4 with longitudinal and lateral distance are used to define a bent area representing the local

road surface and calculate the final track normal vector e_n . The size depends on the tire dimension. The intersection of the rim center plane with the local track plane will now determine the longitudinal and lateral directions e_x and e_y , as well as the geometric contact point P.

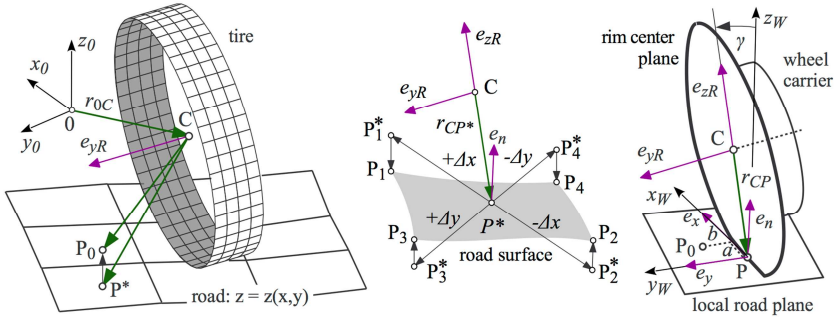


Figure 2: Contact geometry

On a cambered tire, however, the static contact point Q will represent the contact patch more appropriately than the geometric contact point P, Figure 3. Assuming that the pressure distribution on a cambered tire corresponds with the shape of the deflected tire area, the acting point of the resulting vertical tire force F_z is shifted from the geometric contact point P to the static contact point Q. The size of the deflected area corresponds with a generalized vertical tire deflection Δz and its center determines the lateral deviation y_Q of the contact point. The static contact point Q described by the vector $r_{0Q} = r_{0P} + y_Q e_y$ will represent the contact patch very well in any situation, because it is always placed inside the contact area. In contrast, the geometric contact point P as indicated in Figure 3 may even be located outside the contact area in situations where the tire is close to liftoff.

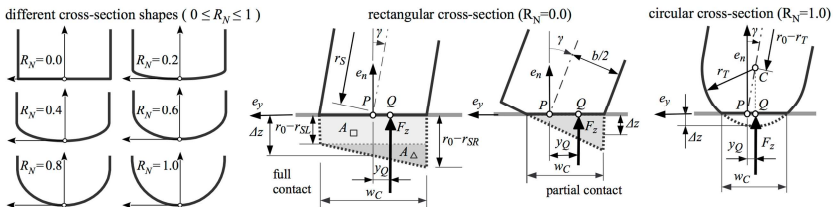


Figure 3: Different tire cross-section shapes and influence on the location of the contact points

The shape of the deflected area strongly depends on the shape of the cross section of the unloaded tire and on the camber angle in addition. Whereas passenger car or truck tires usually have a nearly rectangular cross-section, motor-cycle tires often do have a circular or a more rounded cross-section. Within TMeasy complex shapes of cross-sections are approximated by a simple roundness parameter. The plots on the left side of Figure 3 illustrate how increasing values of the roundness parameter R_N will morph a rectangular cross-section continuously into a circular one.

1.4 Steady-State Forces and Torques

1.4.1 Wheel Load and Tipping Torque

The vertical tire force F_z is calculated as a function of the tire deflection Δz and its time derivative $\Delta \dot{z}$. In a first approximation, the wheel load is separated into a static and a dynamic part,

$$F_z = F_z^{st} + F_z^D = a_1 \Delta z + a_2 (\Delta z)^2 + d_z \Delta \dot{z} \quad (1)$$

where the static part is described as a nonlinear function of the tire deflection and the dynamic part is roughly approximated by a linear damper element. Because the tire can only apply pressure forces to the road, the normal force will be restricted to $F_z \geq 0$. TMeasy replaces the parameter a_1 , a_2 of the parabola by the values of the tire radial stiffness at the payload and double the payload. The tipping torque is taken into account by applying the wheel load F_z at the static contact point Q .

1.4.2 Slips and Forces into Longitudinal and Lateral Directions

The brush model approach used in TMeasy delivers the longitudinal and lateral slips as

$$s_x = \frac{-(v_x - r_D \Omega)}{r_D |\Omega| + v_n} \quad \text{and} \quad s_y = \frac{-v_y}{r_D |\Omega| + v_n} \quad (2)$$

where v_x and v_y are the components of the contact point velocity, r_D is the dynamic rolling radius, and Ω denotes the angular velocity of the wheel about its rotation axis. A small fictitious velocity $v_N > 0$ added to the denominator avoids numerical problems on a locked wheel, where $r_D |\Omega| = 0$ will hold. Please note, that this slip definition is used internal in TMeasy only and may differ from various definitions in the literature.

The longitudinal and the lateral forces are described as functions of the longitudinal and the lateral slips $F_x = F_x(s_x)$ and $F_y = F_y(s_y)$, Figure 4. During general driving situations, e.g., acceleration or deceleration in curves, the longitudinal slip s_x and the lateral slip s_y will appear simultaneously. In order to generate an appropriate combined

force, the longitudinal and lateral slips are normalized, slightly modified, and composed to the combined slip s_C , Figure 4.

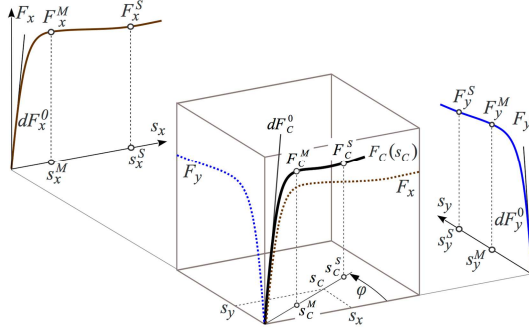


Figure 4: Combined tire forces

The combined tire force characteristic $F_C = F(s_C)$ is defined in TMeasy by characteristic parameters: the initial inclination, the location and the magnitude of the maximum, as well as the sliding limit and the sliding force, Figure 4. These parameters are appropriately derived from the corresponding values of the longitudinal and lateral force characteristics, [3].

1.4.3 Self-Aligning and Bore Torque

The dynamic tire offset or the pneumatic trail mainly depends on the lateral slip, $n = n(s_y)$. Acting as a lever to the lateral force F_y it generates the self-aligning torque.

$$T_s = -n(s_y) \cdot F_y \quad (3)$$

In particular during steering motions, the angular velocity of the wheel has a component perpendicular to the contact patch which is defined as bore motion of the tire. If the wheel moves in the longitudinal and lateral direction too, then a very complicated deflection profile of the tread particles in the contact patch will occur. Within TMeasy the contact patch is substituted for that purpose by a thin ring with the equivalent bore radius R_B . The corresponding bore slip and the bore torque will then be determined by

$$s_B = \frac{-R_B \omega_n}{r_D |\Omega| + v_n} \quad \text{and} \quad T_B = R_B F_C(s_B) \quad (4)$$

where the equivalent bore radius R_B serves as lever arm, $R_B \omega_n$ describes the circumferential sliding velocity and F_C is determined by the combined force characteristic. However, the simple steady-state bore torque model will serve as a rough approxima-

tion only. In particular, it is less accurate at slow bore motions ($s_B \approx 0$) that will occur during parking maneuvers. However, a straightforward extension to dynamic tire forces and a dynamic bore torque will generate realistic parking torques, [5].

1.4.4 Three-Dimensional Slip

In particular during steering maneuvers at standstill, a longitudinal, a lateral, and a bore slip will occur simultaneously. By extending the combined slip s_C defined in Figure 4 with the bore slip s_B to a more generalized and three-dimensional slip

$$s_G = \sqrt{s_C^2 + s_B^2} \quad (5)$$

the effects of the bore motion on the combined tire forces and vice versa can be taken into account. The generalized force characteristic $F_G = F_C(s_G)$ will now provide, by

$$F_C^* = F_G \frac{s_C}{s_G} \quad \text{and} \quad T_B = R_B F_G \frac{s_B}{s_G} \quad (6)$$

a modified combined force and the bore torque in the corresponding parts of the generalized force characteristic. A similar decomposition of the modified combined force finally results in the longitudinal and lateral forces.

1.4.5 First Order Tire Dynamics

The tire forces F_x and F_y acting in the contact patch deflect the tire in the longitudinal and lateral direction, as depicted in Figure 5. In a first-order approximation, the dynamic tire forces follow from

$$F_\diamond^D = F_\diamond(v_\diamond + \dot{\diamond}_e) \approx F_\diamond(v_\diamond) + \frac{\partial F_\diamond}{\partial v_\diamond} \dot{\diamond}_e \quad (7)$$

where $\diamond \in \{x; y\}$ denotes the longitudinal and lateral direction as well as $\dot{\diamond}_e$ names the corresponding tire deflection, respectively.

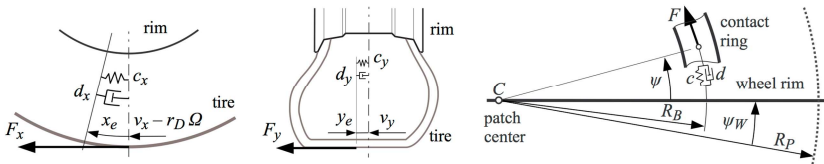


Figure 5: Tire deflection in the longitudinal, lateral and circumferential direction

In steady state the longitudinal and lateral tire forces will be provided as functions of the slips. On the other hand, the dynamic tire forces can be derived from

$$F_x^D = c_x x_e + d_x \dot{x}_e \quad \text{and} \quad F_y^D = c_y y_e + d_y \dot{y}_e \quad (8)$$

where c_x , c_y and d_x , d_y denote stiffness and damping properties of the tire in the longitudinal and lateral direction. Combining the relations in (7) and (8) finally results in first-order differential equations for the longitudinal and lateral tire deflection,

$$(v_{T_x}^* d_x + f_G) \dot{x}_e = -v_{T_x}^* c_x x_e - f_G (v_x - r_D \Omega) \quad (9.1)$$

$$(v_{T_y}^* d_y + f_G) \dot{y}_e = -v_{T_y}^* c_y y_e - f_G v_y \quad (9.2)$$

where $f_G = F_G/s_G$ defines the global derivative of the generalized tire characteristic and modified transport velocities $v_{T_x}^*$ and $v_{T_y}^*$ are used to simplify the expressions.

In a similar approach the dynamic bore torque is modeled by

$$T_B^D = c R_B^2 \psi + d R_B^2 \dot{\psi} \quad \text{with} \quad (10.1)$$

$$[d(r_D |\Omega| + v_n) + f_G] \dot{\psi} = -c \psi (r_D |\Omega| + v_n) - f_G \Omega_n \quad (10.2)$$

where c , d , approximate the circumferential stiffness and damping properties of the tire, ψ describes the torsional deflection of the tire, and Ω_n names the bore angular velocity defined by the component of the wheel angular velocity normal to the road.

By neglecting possible dynamics of the tire offset, the dynamic self-aligning torque can be approximated by

$$T_S^D = -n F_y^D \quad (11)$$

as a product of the steady-state tire offset and the dynamic tire force. In this approach the dynamics of the self-aligning torque is controlled by the dynamics of the lateral tire force only.

This first-order dynamic tire model used in TMeasy is completely characterized by the generalized steady-state tire characteristics f_G , and the stiffness c_x , c_y , c and damping d_x , d_y , d properties of the tire. Via the steady-state tire characteristics, the dynamics of the tire deflections and hence the dynamics of the tire forces and the bore torque will automatically depend on the wheel load F_z and the generalized slip s_G .

2 Parameter Fitting

In this chapter the quantities named with capitals, which, e.g., have to be measured from any (real or virtual) tire test rig, are defined by the TYDEX-format, [4]. At present the tire model TMeasy requires 52 model-parameters in total. Some of them depend on the geometric properties of the tire others may be set automatically. This paper focuses on those TMeasy parameters that have a strong influence on the handling performance of a vehicle. In [5] one can find a detailed explanation of how to get a

valid parameter set even if no tire measurements are available. In fact the manageable amount of physically based parameters is one of the significant advantages of TMeasy in contrast to other (semi-)empirical tire models. The easy parameter handling enables engineers to perform pre-application, even if precise tire information is missing. With more effort, model parameters can also be adjusted to fit tire measurements with high accuracy. A general fitting procedure and, based on this, exemplary results are presented in the following. The actually fitting of dynamic parameters and its validation was performed with the Car Professional package of the simulation framework DYNA4, [6].

2.1 General Procedure

Some exemplary standard test cases to derive the respective model parameters are shown in Table 1. Using an individual characteristic curve, the parameters can either be calculated from this or be adjusted for best possible fit.

First of all, the basic geometry information (No. 1) of the unloaded tire has to be established. Almost all other parameters except the tire roundness factor are wheel load dependent and therefore the subsequent test cases must be carried out at different wheel loads.

The longitudinal, lateral and vertical stiffness (No. 2) can be directly calculated from the respective force-excitation diagrams. In reality the damping properties of a tire are nonlinear especially for high frequencies and are very difficult to measure. Since the influence on low frequency handling maneuvers is not significant, TMeasy contains a linear damping behavior. Because of numerical stability the value of the damping coefficient may not be zero and may not be too big. If loss angle measurement is not available, an initial guess can be derived from the attenuation factor of an oscillation. More tips can be found in [5].

The dynamic rolling radius is an important value, because it is part of the slip definition. It is achieved by measuring the wheel turns and distance covered of a free rolling wheel on a tire test rig or in a car (No. 3), without any inclination or side slip. In TMeasy it is modeled by a linear blending function between the unloaded and loaded tire radius. The weighting coefficient used in this function can be adjusted to fit the characteristic curve properly.

The longitudinal and lateral as well as the self-aligning properties (No. 4 and 5) can be fitted via quasi-static tests based on linear sweeps of the longitudinal slip and the side slip angle, respectively. The latter test case is based on test No. 5.1 and serves as adjustment of the parameters describing the behavior of the pneumatic trail, Figure 6.

#	Test case	Characteristic curve	Model Parameters
1	<i>Tire dimension</i>	<i>NOMWIDTH, ASPRATIO, RIMDIAME</i>	UNLOADED_RADIUS, WIDTH, RIM_RADIUS
2.1	Stiffness & damping	FX vs. LONGDISP	CLONG, DLONG
2.2		FYW vs. LATDISPW	CLAT, DLAT
2.3		FZW vs. DSTWOWHC	CVERT, DVERT
3	Dynamic rolling radius	KROLRAD vs. FZW	RDYNCO
4	Pure longitudinal slip	FX vs. LONGSLIP	DFX0, FXMAX, SXMAX, FXSLD, SXSLD, AMPLFX_<POS,NEG>
5.1	Pure lateral slip	FYW vs. SLIPANGL	DFY0, FYMAX, SYMAX, FYSLD, SYSLD
5.2		MZW vs. SLIPANGL	PT_NORM, SY_CHSI, SY_ZERO
6	Pure bore slip	MZW vs. SLIPANGL	CTORS, DTORS, RB_ADJUST
7.1	Combined camber and bore slip	FYW vs. INCLANGL	CAMF
7.2		MXW vs. INCLANGL	ROUNDNESS
8	Pure long. dynamics	FX vs. RUNTIME	CXDYNC
9	Pure lat. dynamics	FYW vs. RUNTIME	CYDYNC

Table 1: Overview of the TMeasy fitting procedure

In the next step, the parameters of pure bore motion should be determined in a dynamic steering sine-sweep at standstill (No. 6). If no test bench is available, you will find hints in [5] to estimate torsional compliance as well as the bore radius.

In a real car steering and thus cornering as well as tire inclination lead to bore angular velocity and bore slip, respectively. This is why a proper value of RB_ADJUST is needed to determine an influence factor acting on the estimated camber force (No. 7.1). The inclination angle shifts the geometric contact point and thus produces a tipping torque (No. 7.2). Due to a simultaneous influence of the tire roundness on both the camber force and the tipping torque, one could not perform a serial parameter fitting but have to find a pareto optimality instead.

Finally in the dynamic equations (9) the longitudinal and lateral relaxation length can be slightly modified by introducing scaling factors acting on the stiffness quantities, Figure 7. The identification of these parameters in test No. 8 and No. 9 could be done by validation of full vehicle or tire component simulation with measured step response, for example pulsed braking or steering step. Many other parameters influence the dynamic behavior and the simple approximation is not able to simulate mass oscil-

lation. Nevertheless it is precise enough for typical handling maneuvers and the development of driving stability controllers.

The rolling resistance is not important for a handling tire model. Usually it is expressed as the ratio of drag force to wheel load. In the handling model of TMeasy it is calculated as torque $T_y = -\text{sign}(\Omega) f_R r_0 F_z$, where f_R (RRCOEFF) denotes the dimensionless rolling resistance coefficient. More sophisticated equations can be used to overwrite the internal value for high fidelity consumption analysis.

TMeasy specifies the tire characteristics for the nominal or payload FZ_NOM and its double. In normal driving situations the wheel load is mostly smaller than the double payload. Extreme dynamic effects may produce peaks in the wheel load with values exceeding the normal range. To ensure realistic parameter values at all wheel loads, the parameter FZ_MAX is used to limit the wheel load dependent tire parameter interpolation.

2.2 Results

The described fitting procedure was used to generate a TMeasy dataset for a common tire of the automotive mid-sized class. At this point only the lateral tire properties are presented and discussed.

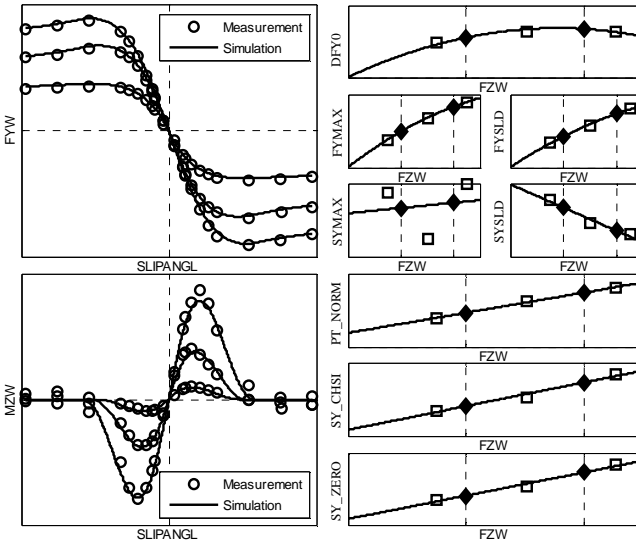


Figure 6: Fitting of lateral force and self-aligning torque parameters (quasi-static)

On the left side in Figure 6 the resulting characteristic curves of self-aligning torque MZW and lateral tire force FYW are shown after parameter fitting No. 5. The preceding step in each case was to identify an optimal parameter set at each wheel load. These values are shown on the right side of Figure 6 by square markers for every model parameter describing the stationary lateral tire properties. In the next step a least square approximation with linear or parabolic trial functions was used to calculate the model parameters at the payload and its double. These final parameters are marked with filled diamond.

In general all parameters related to forces are calculated by a parabolic function (e.g. FYMAX). Here one needs to ensure that the following conditions are fulfilled for each wheel load in the range of $0 \leq F_z \leq FZ_MAX$: $FYMAX \geq FYSLD$, $SYMAX \geq SYSLD$, $SY_ZERO \geq SY_CHSI$. To avoid non-physical behavior FZ_MAX has to be set in such a way, that FYMAX and FYSLD are always increasing in the relevant wheel load range. As one can see in Figure 6, the linear and parabolic trial functions approximate the wheel load individual parameter fitting results quite well. Based on this TMeasy depicts the measured lateral force and self-aligning torque with high accuracy.

An enhanced formulation of the tire dynamics is implemented in DYNA4, [6]. The scaling factor CYDYN C affects the stationary lateral stiffness and therefore the so called lateral relaxation length. Here this quantity is identified on the basis of side slip angle steps at different wheel loads. The steering gradient is approximately 60°/s. On the left side of Figure 7 the time-based course of the lateral force at a wheel load nearby payload is shown. As depicted on the right side of Figure 7, a linear curve fit of the wheel load specific optimal parameter values is suitable. The dashed horizontal line indicates scale 1, which means that here the dynamic has to be slightly faster than originally calculated with eq. (9). This leads to an accurate dynamic response both in the step up and step down phase. Simulations at other loads yield similar results.

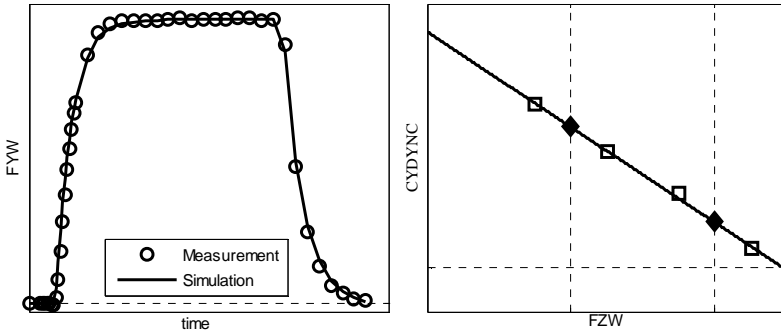


Figure 7: Lateral step response and parameter fitting (dynamic)

3 Optimization and Validation

In the presented particular example the tire test rig measurement procedure No. 7 from Table 1 was not available, whereby for the parameters describing the bore motion behavior only default ($RB_ADJUST = 1$) or approximated ($CTORS \approx 2500$ N/m and thus $DTORS \approx 3$ Ns/m) values could be set initially. Especially the latter parameters are based on simple assumptions and will serve as a very first guess, if no measurements or additional information are available, [3].

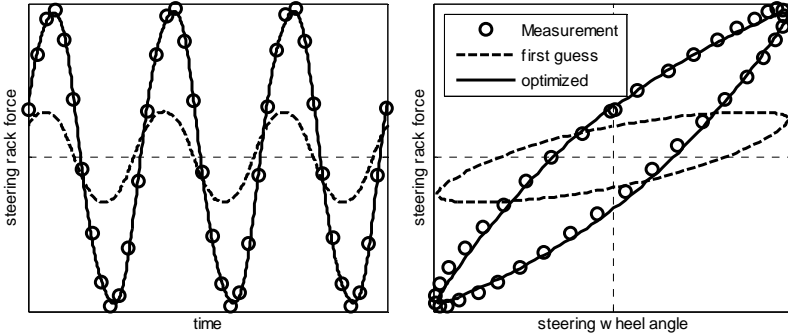


Figure 8: Sinusoidal steering input at standstill compared to full vehicle measurement

For this specific tire, a matching concerning the steering rack force extracted from a full vehicle measurement opens the opportunity to adjust the initial guess of the mentioned parameters. In Figure 8 the results of a sinusoidal steering with constant amplitude and frequency at standstill are depicted. Regarding its magnitudes, this might be especially interesting for rear steering scenarios. Here one can see a smaller amplification and a phase shift in the simulation results of the initial parameter set (dashed lines) compared to the measurement. In this test case the influence on these characteristics of both the bore radius adjustment factor and the torsional stiffness is shown in Figure 9. The diagrams contain also both the target amplification and target phase calculated from the measurement and thus all valid parameter sets $\{RB_ADJUST; CTORS\}$ leading to these targets via the level curves. Due to its minimal influence on the bore dynamics, the parameter $DTORS$ is calculated as solely depending on $CTORS$. Now one gets a realistic parameter set by the intersection of those level curves, what finally leads to $RB_ADJUST \approx 0.95$ and $CTORS \approx 7000$ N/m. Therefore the bore radius adjustment factor seems to be very well estimated by the model itself, whereas the torsional stiffness needs to be significantly greater. In general, higher stiffness produces faster first order dynamics, thus a higher corner frequency and less

damping of the input amplitude, respectively. As depicted in Figure 8 by the solid line, simulating with this adjusted parameter set results in a high congruence regarding the measured steering rack force.

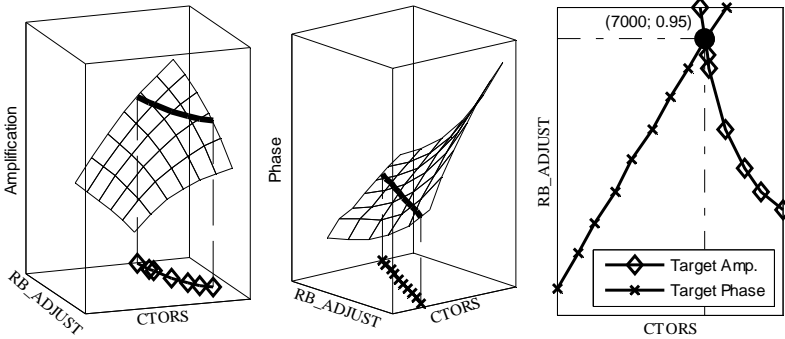


Figure 9: Parameter adjustments to improve bore motion behavior

For validation a comparison of the torque around the z_W -axis MZW in a lateral step response test on the tire test rig is shown in Figure 10. One can see, that the bore torque T_B dominates the sum of torques (solid line) most of the steering phase (i.e. where $T_B \neq 0$ holds) and generates a characteristic peak. Simulating with the just derived parameter set depicts this behavior very well. In the dynamic phase the self-aligning torque T_S increases and reaches its stationary value, which draws to the measured end value.

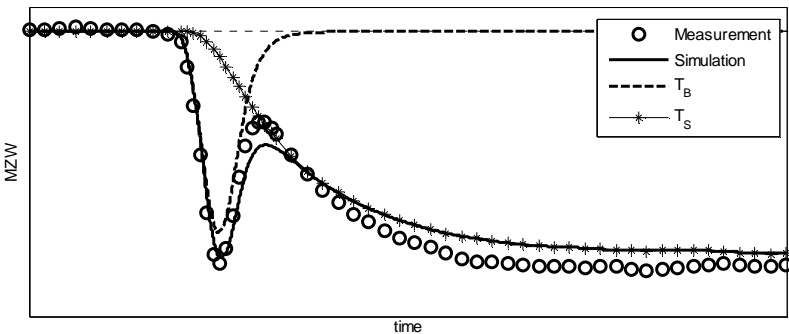


Figure 10: Self-aligning torque at a step response test on the tire test rig

4 Conclusion

The present paper describes the general approach of the semi-physical tire model TMeasy for vehicle dynamics and handling simulation and its enhancement for bore torque simulation in Version TMeasy 5. A parameter fitting process realized by TESIS DYNAware and the validation of real tire behavior by simulation with DYNA4 is presented.

Even with first guess parameters, the TMeasy tire model behaves in a realistic and plausible manner. Parameter estimation is intuitive and datasets from previous model versions can be easily migrated. After parameter fitting, the simulation results correlate well with both the tire test rig and full vehicle measurements. The enhancement of a three-dimensional slip calculation in the latest version does not modify the model behavior for high slip conditions, but improves the results not only for highly dynamic situations but also for low speed maneuvers such as parking.

References

1. G. Rill, An engineer's guess on tyre parameter made possible with TMeasy, in: Proceedings of the 4th International Tyre Colloquium (P. Gruber and R. S. Sharp, eds.), (University of Surrey, GB), 2015.
2. W. Hirschberg, F. Palacek, G. Rill and J. Sotnik, Reliable Vehicle Dynamics Simulation in Spite of Uncertain Input Data, Proceedings of 12th EAEC European Automotive Congress, Bratislava, 2009.
3. G. Rill, Road Vehicle Dynamics, Fundamentals and Modeling, Taylor & Francis, Boca Raton, 2011
4. H.-J. Unrau, J. Zamow, TYDEX-Format, release 1.3, TYDEX Workshop, 1997, retrieved January 13, 2016, https://www.fast.kit.edu/download/DownloadsFahrzeugtechnik/TY100531_TYDEX_V1_3.pdf
5. Georg Rill. An engineer's guess on tyre parameter made possible with TMeasy. In P. Gruber and R. S. Sharp, editors, Proceedings of the 4th International Tyre Colloquium, University of Surrey, GB, 2015.
6. <http://www.thesis-dynaware.com> (retrieved January 13, 2016)